JACS Au
AN OPEN ACCESS JOURNAL OF THE AMERICAN CHEMICAL SOCIETY

pubs.acs.org/jacsau
Article

General Platform for Efficient and Modular Assembly of GalNAc–siRNA Conjugates via Primary Amines and *o*-Nitrobenzyl Alcohol Cyclization Photoclick Chemistry Enabling Rapid Access to Therapeutic Oligonucleotides

Hui-Jun Nie,[#] Hao Hu,[#] Xinming Qi,[#] Yin-Jue Zhou, Lu Liu, and Xiao-Hua Chen*

Cite This: *JACS Au* 2025, 5, 1402–1412

Read Online

ACCESS | Metrics & More | Article Recommendations | Supporting Information

ABSTRACT: Oligonucleotide-based therapies, especially ligand-conjugated siRNAs, offer significant therapeutic potential for a wide array of diseases. However, conventional solid-phase synthesis and current postsynthetic in-solution conjugation methods face notable challenges related to efficiency, accessibility, and the scalability of diverse ligand–oligonucleotide conjugates. Herein, we introduce a novel strategy for highly efficient, rapid, and modular assembly of GalNAc–siRNA conjugates based on light-induced primary amine and *o*-nitrobenzyl alcohol cyclization (PANAC) chemistry. Leveraging the advantages of PANAC photoclick chemistry and modular conjugation linkers, our method enables the direct assembly of trivalent GalNAc (tGalNAc) with commercially available primary-amine-modified siRNAs. This approach demonstrates the efficient and rapid assembly of therapeutically relevant oligonucleotides with ligands of interest, offering operational simplicity and practicality; thus, it effectively overcomes the limitations of existing methods. More importantly, the developed siRNA–tGalNAc conjugates showed a robust gene silencing effect superior to the parent siRNA conjugate, highlighting the effectiveness of our method in generating and screening siRNA conjugates to enhance in vivo potency. Overall, our method enables modular and rapid assembly of therapeutically relevant oligonucleotide–tGalNAc conjugates using readily accessible oligonucleotides and commercially available tGalNAc-amine ligands. This approach expands the toolkit for generating ligand–oligonucleotide conjugates, providing a general and efficient platform with broad applicability, thereby advancing the optimization and development of oligonucleotide-based therapeutics.

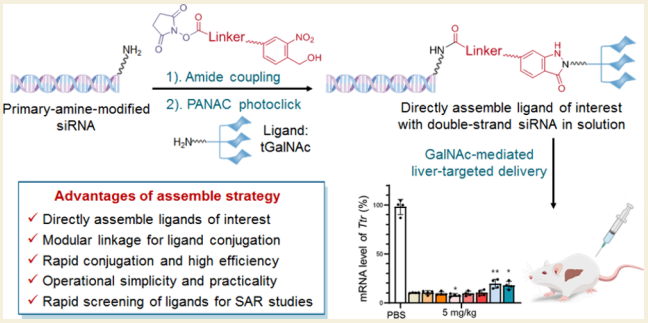

KEYWORDS: *RNA therapeutics, GalNAc–siRNA conjugates, Therapeutic oligonucleotide, Photoclick chemistry, Modular assembly*

INTRODUCTION

Oligonucleotide-based therapies have emerged as a promising approach for the treatment of a variety of genetic diseases, with a growing number of approved drugs and a substantial pipeline of molecules in clinical trials.[1−4] By targeting specific mRNA or DNA sequences, oligonucleotides can precisely regulate gene expression to modulate the function of disease-related genes, leading to therapeutic effects.[3] Small interfering RNA (siRNA) is a key type of oligonucleotide therapeutics, typically consisting of short, double-stranded RNA molecules that can specifically bind target mRNA. The mechanism of action of siRNA relies on its high complementarity and affinity to RNA targets, which induce the degradation of the bound mRNA, thereby effectively suppressing the expression of target genes.[5] siRNA therapies have shown significant efficacy in treating diseases, including genetic and rare diseases, cardiovascular diseases, hereditary eye disorders, neurological disorders, hypercholesterolemia, cancer, viral infections, etc.[5,6] Thus, siRNAs hold broad clinical potential for various therapeutic applications, with multiple approved drugs (Figure 1a) and many preclinical and clinical trials in process.[6]

Despite the immense potential of siRNA therapies in disease treatment, several challenges remain in their development. The main hurdles include inadequate delivery to specific tissues causing unintended tissue side effects, poor metabolic stability leading to rapid degradation in the body, and compromised cellular uptake resulting in low bioavailability.[5,6] To address these issues, various chemical modification strategies (e.g., backbone modification, sugar modification, or conjugation with ligands) are developed, which have significantly enhanced the targeting capability, metabolic stability, and cellular uptake

Received: January 6, 2025
Revised: February 11, 2025
Accepted: February 11, 2025
Published: February 24, 2025

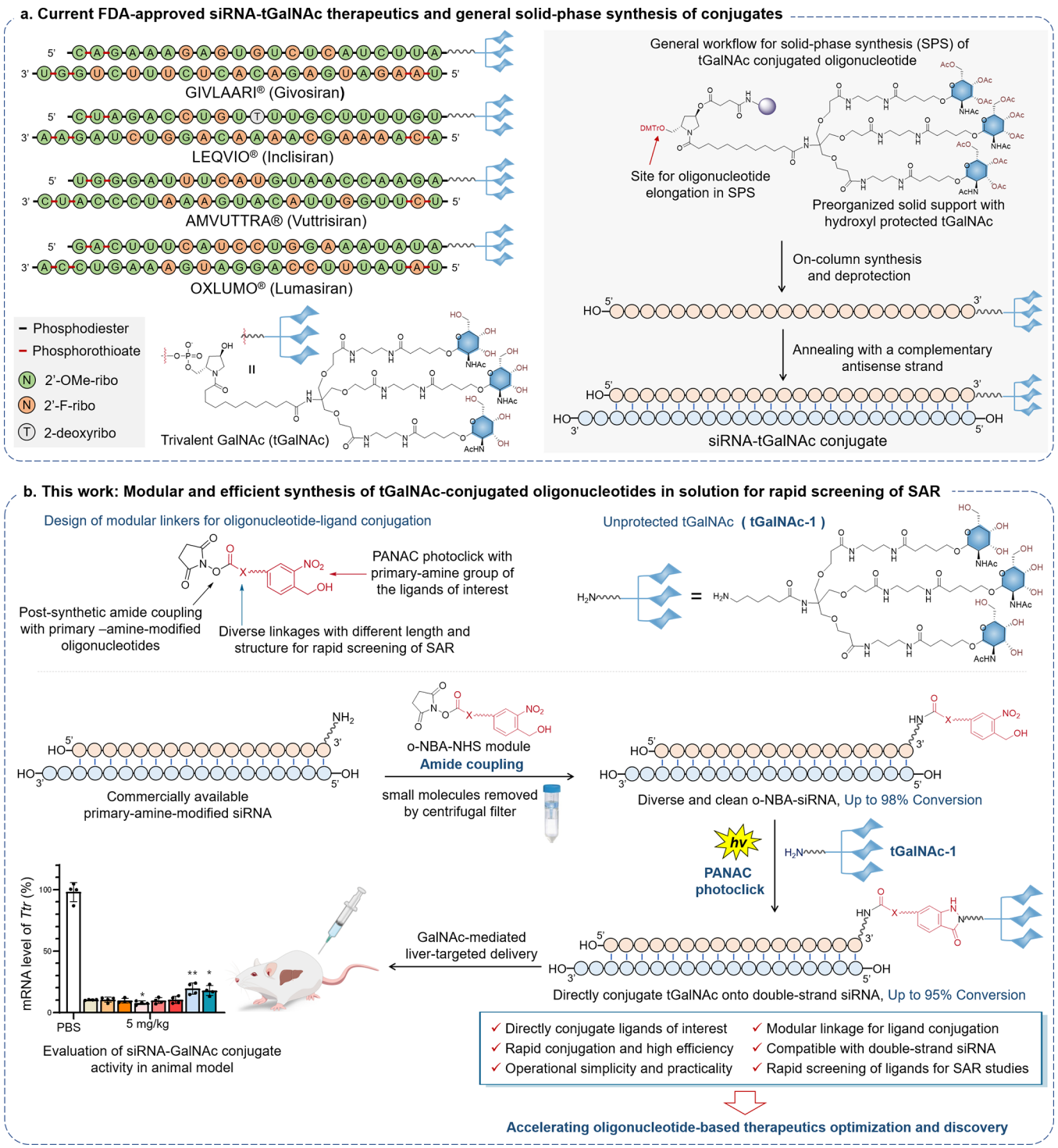

Figure 1. Schematic representation of siRNA−tGalNAc therapeutics and general method for assembly of these conjugates and the design of our strategy. a) FDA-approved siRNA−tGalNAc therapeutics and the workflow of solid-phase synthesis of siRNA−tGalNAc conjugates. b) This work. PANAC photoclick chemistry-enabled modular and efficient assembly of tGalNAc-conjugated oligonucleotides to enhance *in vivo* potency and the advantages of direct assembly strategy.

of siRNA.[4−6] Particularly, the development of a variety of ligand (e.g., lipids, peptides, antibodies, aptamers, and GalNAc) conjugated siRNAs has provided a promising solution to improve cellular uptake and target delivery, thus optimizing the therapeutic outcomes.[5,7,8] Among others, siRNA−GalNAc conjugates stand out as one of the most important types (Figure 1a). The GalNAc conjugates have shown high affinity and specificity targeting the ASGPR (asialoglycoprotein receptor) on liver cells and prompt cellular uptake through endocytosis, thus leading to efficient liver-specific delivery of the siRNA therapeutics and robust gene silencing.[9−11] Of the six FDA-approved siRNA therapeutics, five are siRNA−GalNAc conjugates, with several more in clinical trials, highlighting their substantial clinical value.[6,10,12]

Currently, the most widely used strategy for constructing siRNA−ligand and siRNA−GalNAc conjugates is attaching a

https://doi.org/10.1021/jacsau.5c00012
JACS Au 2025, 5, 1402−1412

ligand of interest or trivalent GalNAc (tGalNAc) moiety to the 3′-end of the sense strand siRNA, as exemplified by approved therapies (such as Givosiran, Lumasiran, Inclisiran, and Vutrisiran, Figure 1a) as well as other novel siRNA−tGalNAc conjugates in clinical trials or preclinical investigations.[1,4,10,12−14] Oligonucleotide−tGalNAc conjugates are typically prepared by solid-phase synthesis (SPS). In this method, a tGalNAc linker is preorganized on a solid support, on which the oligonucleotide is elongated in a 3′ to 5′ direction (Figure 1a, right panel).[14−16] Nonetheless, the steric hindrance of the bulky and branched tGalNAc linker often leads to suboptimal coupling efficiency and the accumulation of various byproducts during the nucleotide elongation cycles, which result in compromised yields and complex purification processes, further driving up the production costs of siRNA therapeutics.[13,17,18] Additionally, with regard to the increasing demand for oligonucleotides (driven by their expanding therapeutic applications), the sustainability challenges and the limited scalability of automated solid-phase synthesis pose significant pressure on the global healthcare system.[3] Moreover, even small variations in the ligands of interest and their linkages require the use of a newly preassembled solid support for on-column synthesis of siRNA−ligand conjugates in each new SPS experiment.[17] Consequently, this requirement significantly restricts the efficiency and accessibility to rapidly screen structure−activity relationships (SARs) using the same siRNA sequence backbone for targeting the same mRNA.

Alternatively, postoligonucleotide-synthesis coupling in solution allows for the construction of conjugates after the oligonucleotide has been synthesized. This strategy not only offers improved coupling efficiency and scalability to reduce the production cost but also provides greater chemical versatility and accessibility to enable facile production of diverse conjugates on the same oligonucleotide to facilitate SAR studies.[13,19,20] Recently, several in-solution postsynthetic conjugation methods are developed, but they more or less have some limitations, such as the activated ester-based amide formation relying on SPS building blocks that are not commercially available,[13] tandem copper-catalyzed click synthesis using toxic metal catalysts,[19,21] copper-free strain-promoted azide−alkyne cycloaddition (SPAAC) reaction that generates chiral center complexing subsequent purification,[22] native chemical ligation (NCL),[20] and thiol−ene click[23] reaction resulting in moderate yield in some cases. Moreover, most of these studies primarily focused on assessing the chemical feasibility of the new coupling methodologies, without thoroughly evaluating the impact of these developed linkages on the biological activity, particularly *in vivo* antisense activity, of oligonucleotide−tGalNAc conjugates.[19,20] Therefore, developing innovative conjugation strategies that enhance the efficiency and accessibility of the direct construction of siRNA−GalNAc conjugates while ensuring the scalability of diverse siRNA−ligand conjugates is crucial for advancing oligonucleotide-based therapeutics and fully realizing their therapeutic potential.

We present here a novel and versatile platform for rapid access to siRNA−ligand conjugates, utilizing our recently developed PANAC photoclick chemistry[24−26] to enable the high-efficiency, rapid, and modular assembly of tGalNAc with commercially available primary-amine-modified siRNAs (Figure 1b). We designed modular and different linkers by integrating *o*-nitrobenzyl alcohol with *N*-hydroxysuccinimide (NHS) ester, demonstrating the versatility and accessibility of our method for the direct assembly of therapeutically relevant tGalNAc conjugate oligonucleotides. This direct assembly strategy offers operational simplicity and practicality for the efficient and modular construction of diverse GalNAc−siRNA conjugates, effectively overcoming the limitations of conventional solid-phase synthesis and other in-solution postsynthetic methods. More importantly, using this strategy, the generated siRNA−tGalNAc conjugates targeting the mouse transthyretin (Ttr) gene demonstrated comparable or superior activity compared to the reported positive control,[27] highlighting the potential of this approach for the development of effective siRNA-based therapeutics (Figure 1b). Overall, our strategy expands the toolbox for siRNA−tGalNAc conjugation and provides a general platform for the efficient and rapid assembly of diverse siRNA−ligand conjugates, accelerating the optimization of conjugates with the desired biological activity and advancing the development of oligonucleotide-based therapeutics.

EXPERIMENTAL SECTION

General Method for the Synthesis of Linker

For the synthesis of linker 1, *N*,*N*-diisopropylethylamine (DIPEA) (1.8 mL, 10.29 mmol) was added to a solution of Compound **2** (800 mg, 3.43 mmol), Compound **1a** (676 mg, 3.43 mmol), and hexafluorophosphate azabenzotriazole tetramethyl uronium (HATU) (1.3 g, 3.43 mmol) in dry DMF (20 mL). The reaction mixture was stirred at room temperature for 2 h. The reaction mixture was added to water (30 mL) and extracted with ethyl acetate (EtOAc) (2 × 50 mL). The combined organic layers were washed with brine (4 × 40 mL). The resulting organic phase was dried over Na_2SO_4 and filtered. The filtrate was concentrated under a reduced pressure. The residue was purified by chromatography on silica gel with dichloromethane/methanol as the eluent to afford **3a** as a yellow oil (922 mg, 73%). ^{1}H NMR (500 MHz, $CDCl_3$) δ: 8.48 (d, J = 1.7 Hz, 1H), 8.07 (dd, J = 8.1, 1.7 Hz, 1H), 7.79 (d, J = 8.1 Hz, 1H), 7.52 (s, 1H), 4.99 (s, 2H), 3.70 (t, J = 5.7 Hz, 2H), 3.66 (d, J = 2.2 Hz, 4H), 2.49 (t, J = 5.7 Hz, 2H), 1.39 (s, 9H). ^{13}C NMR (126 MHz, $CDCl_3$) δ: 171.96, 165.57, 147.14, 140.43, 134.65, 132.35, 129.35, 123.82, 81.35, 69.08, 65.89, 61.87, 39.90, 35.87, 28.10.

To a solution of **3a** (368 mg, 1 mmol) in dichloromethane (5 mL) was added trifluoroacetic acid (2 mL). The reaction mixture was stirred at room temperature for 3 h. Then the solvent was evaporated *in vacuo* to afford the corresponding carboxylic acid for the next step without further purification. Then, the intermediate described above (1 mmol) was redissolved in 5 mL of dichloromethane. *N*-Hydroxysuccinimide (127 mg, 1.1 mmol), triethyl amine (TEA) (278 μL, 2 mmol), and 1-ethyl-3-(3-(dimethylamino)propyl)-carbodiimide (EDCI) (230 mg, 1.2 mmol) were added. The reaction mixture was stirred at room temperature for 4 h. The completion of the reaction was monitored by LC-MS. The reaction mixture was added to water (15 mL) and extracted with dichloromethane (2 × 30 mL). The combined organic layers were washed with brine (4 × 40 mL). The resulting organic phase was dried in Na_2SO_4 and filtered. The filtrate was concentrated under reduced pressure. The residue was purified by preparative TLC to afford the Linker 1 brown oil (266 mg, 65%) for the next step without further purification. ^{1}H NMR (500 MHz, $CDCl_3$) δ 8.48 (d, J = 1.8 Hz, 1H), 8.20 (dd, J = 8.1, 1.8 Hz, 1H), 7.84 (d, J = 8.1 Hz, 1H), 7.47 (s, 1H), 5.02 (s, 2H), 3.85 (t, J = 5.6 Hz, 2H), 3.70−3.68 (m, 4H), 2.90−2.83 (m, 6H). ^{13}C NMR (126 MHz, $CDCl_3$) δ: 169.76, 167.34, 165.25, 147.16, 139.90, 134.93, 133.58, 129.69, 123.59, 70.00, 65.90, 62.25, 40.17, 32.79, 25.79. HRMS (ESI-Q-TOF): calcd. for $C_{17}H_{20}N_3O_9$ $[M + H]^+$ 410.1194, found 410.1198.

General Synthesis of Oligonucleotide-Linker-tGalNAc

To 8 volumes of reaction buffer ((25 mM Na-Pi)/DMSO = 1:1, pH 10.5) was added 1 volume of oligonucleotide (10×, in 25 mM Na-Pi

https://doi.org/10.1021/jacsau.5c00012
JACS Au 2025, 5, 1402−1412

Scheme 1. Design of Modular Linkers for Conjugation and Synthesis of Linkers 1−3 for Assembly of siRNA−tGalNAc Conjugates[a]

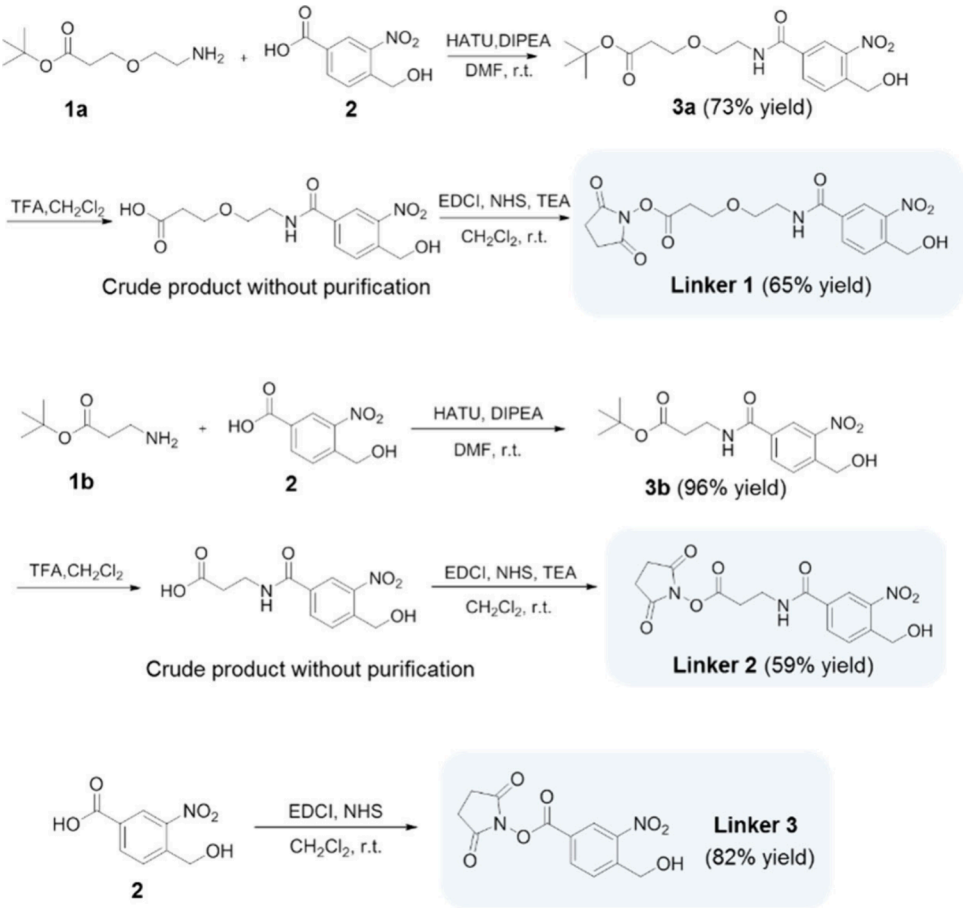

[a]Yield for isolated yield.

solution, pH 8.5) and 1 volume of linker (10× , in DMSO). The reaction mixture was shaken at room temperature for 1 h. The reaction mixture was diluted by ddH_2O to reduce the DMSO concentration to <5% and subjected to ultrafiltration using an Amicon Ultra-0.5 mL centrifugal filter (3k-cutoff, Millipore, cat # UFC5003BK) at 13000*g* for removal of small molecules and buffer-exchange to photoclick reaction buffer (25 mM Na-Pi, pH 8.5). The mixture was transferred to 96-well plate, and tGalNAc (20×) was added. The plate (with lid off) was placed on ice and exposed to 365 nm irradiation (ZF-7A UV lamp, 16 W) at 10 mm distance for 15 min. The samples were collected and incubated at 25 °C for 1 h, followed by LC-MS analysis using a Titank C18 column (3 μm, 50 × 2.1 mm) connected to an Agilent 1260 infinity II HPLC coupled with an Agilent 6230 QTOF-MS. For large-scale preparation of siTtr−tGalNAc conjugates, samples were further purified using a Poroshell HPH-C18 column (4 μm, 150 × 4.6 mm), lyophilized and reconstituted with phosphate-buffered saline (PBS). The concentrations of conjugates were determined with a microspectrophotometer.

In Vivo Gene Silencing Experiment

C57BL/6 male mice aged 6−7 weeks (n = 4 per group) were administered subcutaneously using a volume of 0.1 mL/10 g of body weight. siRNA was administrated in three doses of 0.5, 1.5, and 5 mg/kg for all compounds. The control group was treated with PBS (n = 4). Liver tissues were collected at 120 h postdosing and cryopreserved in −80 °C. An amount of 20 mg of frozen mouse livers was ground and resuspended in 1 mL of Trizol. Chloroform (100 mL) was added to each sample, which was mixed and then incubated at room temperature for 5 min. Samples were centrifuged at 12000*g* at 4 °C for 15 min. The aqueous phase was transferred to a new tube followed by the addition of 1.5 vol of 100% isopropanol. RNA was purified using an EZ-10 spin column. RNA concentration and purity were measured with a NanoDrop. cDNA was synthesized from 500 ng of total RNA per sample using the Hifair AdvanceFast first Strand cDNA Synthesis kit. Real-time qPCR was performed using a Hieff qPCR SYBR Master Mix on a ABI7500 Fast Real Time PCR System. The following qPCR program was used: preincubation for 5 min at 95 °C, 40 cycles of 10 s at 95 °C, 30 s at 60 °C. The relative abundance of transthyretin (Ttr) mRNA was determined by comparison with the internal reference gene glyceraldehyde 3-phosphate dehydrogenase (Gapdh) using the ddCt method. The following primers were used in qPCR: mTtr (Forward primer: 5- TTGCCTCGCTGGACTGGTA-3, Reverse primer: 5-TTACAGCCACGTCTACAGCAG-3), mGapdh (Forward primer: 5- TGACCTCAACTACATGGTCTACA-3, Reverse primer: 5- CTTCCCATTCTCGGCCTTG-3).

RESULTS AND DISCUSSION

Design of Direct Assembly Strategy for Ligand−siRNA Conjugates Based on PANAC Photoclick Chemistry

We have recently developed PANAC photoclick chemistry[24−26] as a versatile and efficient tool for the modular functionalization of a wide range of primary amine-containing molecules, using primary amines as direct and general photoclick handles. Upon light activation, the inert *o*-nitrobenzyl alcohol (o-NBA) moiety is converted into a reactive *o*-nitrosobenzaldehyde intermediate, which then directly reacts with primary amines to form the indazolone

https://doi.org/10.1021/jacsau.5c00012
JACS Au 2025, 5, 1402−1412

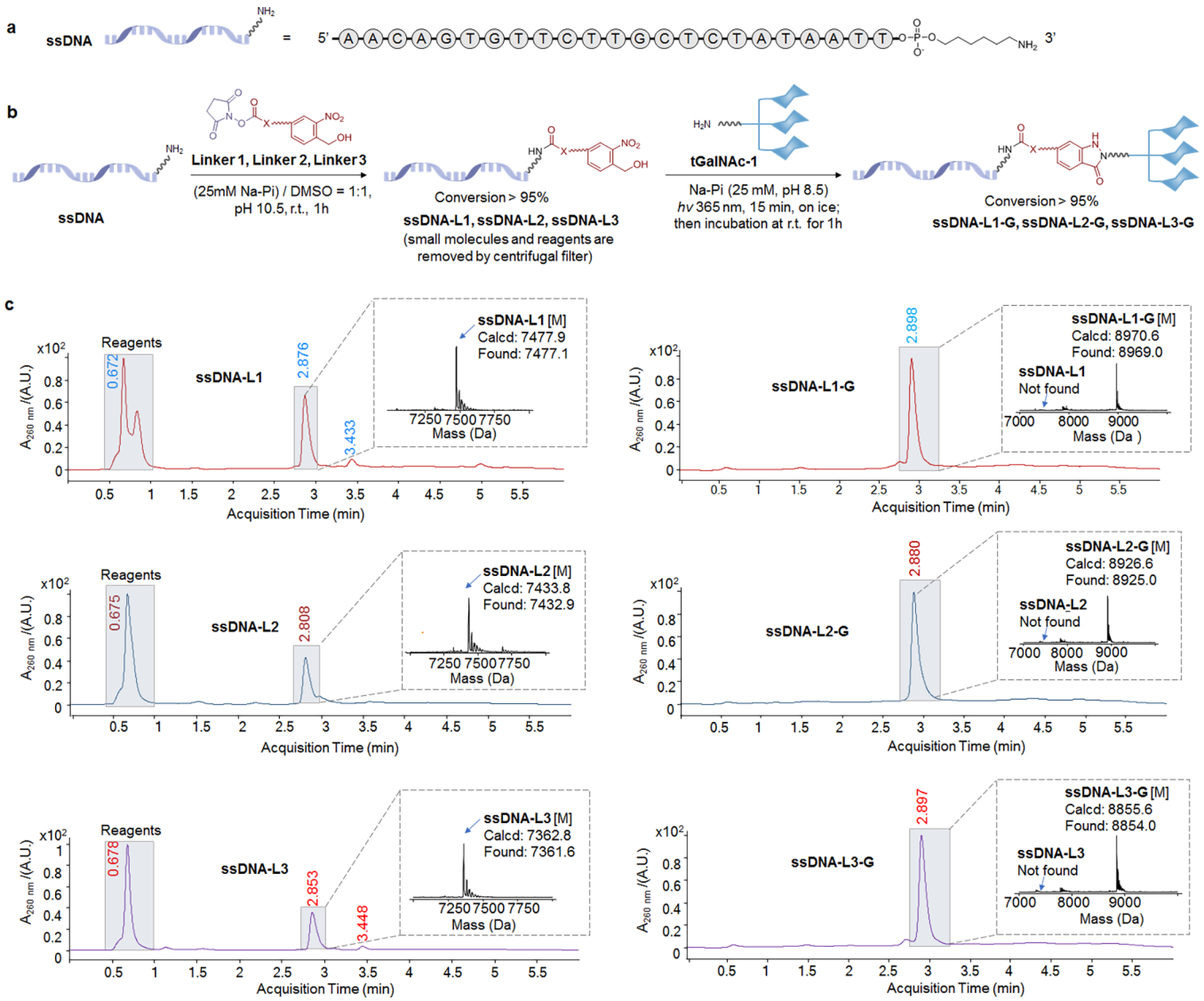

Figure 2. Direct assembly of ssDNA and tGalNAc. a) Sequence and structure of the model aminoalkyl-modified ssDNA. b) Aminoalkyl-modified ssDNA sequentially reacts with linkers and **tGalNAc-1**. Na-Pi, sodium phosphate buffer. r.t., room temperature. c) UPLC analysis of the crude reaction products. Inset: deconvoluted MS spectra of the main peaks. Since the retention times of the starting ssDNA, ssDNA-Linkers and the final ssDNA−tGalNAc conjugates are very similar, the conversion was calculated based on the MS analysis.

scaffold. This process generates stable conjugates without the need for toxic metal catalysts or reagents, ensuring operational simplicity and practicality under mild conditions. The PANAC photoclick chemistry offers high chemoselectivity, easy access to a broad range of primary amine-containing reactants, and fast kinetics, enabling rapid and efficient conjugation even at low reactant concentrations. Additionally, the resulted artificial linkage is achiral (compared to e.g. SPAAC),[22] thereby eliminating stereochemical complexity and simplifying downstream purification processes. Leveraging these advantages, we and other research groups have employed PANAC photoclick chemistry for the modular functionalization of a wide range of small molecules,[28−30] biomolecules,[24−26,31−36] and biomaterials.[37−40]

Building on these advancements, we hypothesized that PANAC photoclick chemistry could enable the in-solution assembly of siRNA with ligands of interest, such as the widely used tGalNAc moiety, facilitating the modular and straightforward generation of stable conjugates with high efficiency in reaction buffer. Since primary amines are among the most synthetically accessible fragments for both siRNA and ligands, we devised conjugation linkers by integrating the *o*-NBA moiety with NHS ester (Figure 1b), considering NHS ester is one of the most extensively used functionalities efficiently reacting with primary amine.[41] We envisioned that the *o*-NBA−NHS modules would first react with the primary amines of siRNA to form *o*-NBA−siRNA conjugates through amide coupling, with NHS as a byproduct that could be easily removed by filtration. Subsequently, the *o*-NBA−siRNA conjugates would undergo a PANAC photoclick reaction with the primary amine of the ligand moieties (e.g., tGalNAc), resulting in the formation of siRNA−tGalNAc conjugates and producing only two molecules of water as byproducts. Therefore, the *o*-NBA−NHS modules act as ideal linkers, enabling the modular and straightforward assembly of stable siRNA−tGalNAc conjugates with the absence of apparent byproducts.

https://doi.org/10.1021/jacsau.5c00012
JACS Au 2025, 5, 1402−1412

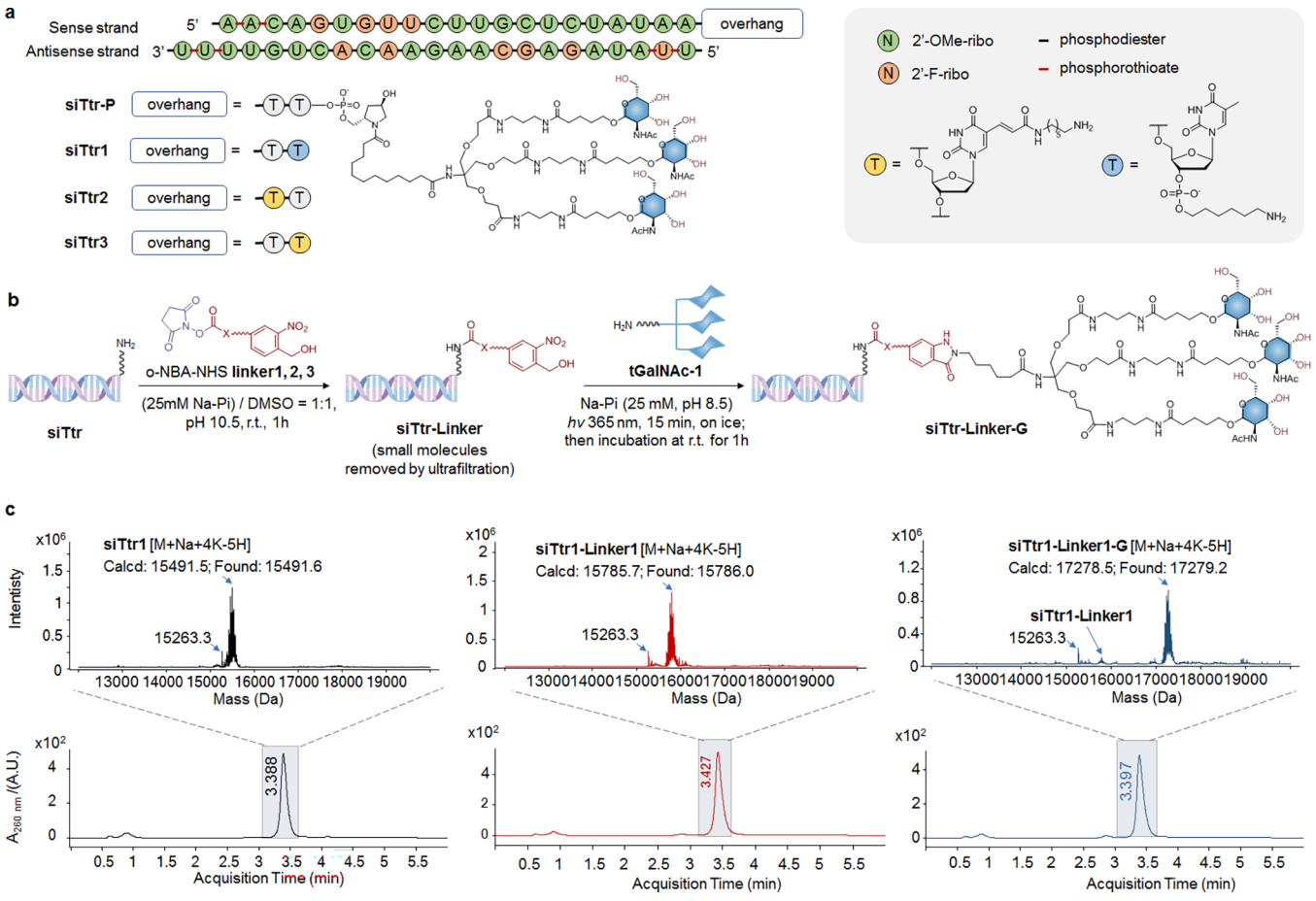

Figure 3. Two-step conjugation of double-stranded siTtr and tGalNAc. a) Sequences and structures of the investigated siRNA molecules. **siTtr-P** is a positive control with verified Ttr-targeting activity. **siTtr1−3** are Ttr-targeting siRNA with an aminoalkyl chain at different positions of 3′-ends of sense chains. b) siTtr molecules sequentially reacting with linkers and **tGalNAc-1**. Na-Pi, sodium phosphate buffer. r.t., room temperature. c) Representative LC-MS analysis of the starting **siTtr1**, **siTtr1-Linker1** crude product (after ultrafiltration), and **siTtr1-Linker1-G** crude product, for Table 1, entry 10, and Table 2, entry 1, respectively. In MS spectra, the signals at m/z 15263.3 represent the peaks of the antisense strand (M*2) of **siTtr1**, **siTtr1-Linker1**, and **siTtr1-Linker1-G**.

Synthesis of Modular Linkers for Direct Assembly of Primary-Amine-Modified siRNAs and tGalNAc

As a proof-of-concept study, we sought to demonstrate the applicability of our coupling strategy by synthesizing siRNA−tGalNAc conjugates targeting the mouse *Ttr* gene and evaluating their biological activities.[14,15] Transthyretin (TTR) protein is produced in the liver; mutated TTR leads to the formation of abnormal fibrils that deposit in peripheral tissues, causing neuropathy and/or cardiomyopathy.[1,3,42] Notably, there are four (out of 22) FDA-approved oligonucleotide-based therapeutics targeting the *TTR* gene, underscoring its clinical significance.[1,3] Accordingly, the mouse *Ttr* gene and corresponding siRNA have been widely used as a model system for developing and validating RNA-based conjugation strategies.[13−15]

To investigate the linker effect of length and rigidity on the coupling efficiency and biological activity, we designed three linkers in which the NHS esters and *o*-NBA moieties are connected with different spacers. The linkers were readily prepared via routes shown in Scheme 1. For Linker 1 and Linker 2, amines **1a, b** were reacted with *o*-NBA-containing carboxylic acid **2** under standard HATU-assisted coupling. The generated amides **3a, b** were subjected to removal of *tert*-butyl groups (deprotection) and coupling with NHS to form active esters in decent isolation yields (65% and 59%, respectively). For Linker 3, acid **2** was coupled with NHS in a one-step reaction with ∼82% isolation yield.

Developing the Direct Assembly Strategy for Single-Stranded DNA Oligonucleotide−tGalNAc Conjugation

First, we investigated the *o*-NBA-NHS linker-mediated oligonucleotide−tGalNAc conjugation using single-stranded DNA (ssDNA) molecules as models due to their stability and chemical simplicity compared to siRNA molecules. We designed an ssDNA molecule corresponding to the sense chain of the reported model siRNA targeting mouse *Ttr* gene,[13−15,27] with an amino-containing alkyl chain appended at the 3′-end (Figure 2a) which is the commonly used site for conjugating with tGalNAc (Figure 1a). The ssDNA is readily prepared via a standard protocol of solid-phase oligonucleotide synthesis, using commercially available aminoalkyl-containing building blocks. In these model reactions, we employed the ssDNA at a submillimolar level (100 μM) to assess the coupling efficiency. For the first-step amide coupling, the ssDNA was incubated with 50 equiv of linker for 1 h at room temperature, in 20 μL of DMSO/Na-Pi buffer which improves the solubility of both reagents (Figure 2b). To our delight, the ultraperformance liquid chromatograph mass spectrometry

https://doi.org/10.1021/jacsau.5c00012
JACS Au 2025, 5, 1402−1412

(UPLC-MS) analysis of all 3 reactions (ssDNA with 3 linkers) showed the products as the only main peaks, with no detectable starting ssDNAs and other overcoupling adducts (e.g., coupling with amines on nucleobases or hydroxyl groups on sugars) or other byproducts observed (Figure 2c). These results suggested the amide coupling achieved almost quantitative and clean conversion.

Then, ultrafiltration was performed to remove small molecules a by centrifugal filter and replace the solvent with PBS buffer (25 mM Na-Pi, pH 8.5). Without further purification, the 3 ssDNA-linker conjugates were subjected to PANAC conjugation with 5 mM **tGalNAc-1** (15 μL reaction mixture). The reaction mixture was placed on ice and subjected to light activation by a hand-held UV lamp (365 nm) at 10 mm distance for 15 min and then incubated at room temperature for 1 h. LC-MS analyses confirmed the complete absence of ssDNA-linkers, with the desired ssDNA−tGalNAc conjugates being the only major products (Figure 2c, right panel). Notably, the high conversion was achieved even for the structurally compact and rigid Linker 3, with no flexible spacer between the *o*-NBA moiety and NHS ester. Additionally, to show that the synthetic route is well-compatible to a cyclic spacer-containing linker, we synthesized a linker containing a piperidine ring (Linker 4), which also exhibited high conversion in the two-step ssDNA−L4-G conjugation (Supporting Information Figure S20). Taken together, these results suggest that our direct assembly strategy enables the efficient and rapid conjugation of tGalNAc to model ssDNA molecules by in-solution postsynthesis conjugation via amide coupling and PANAC photoclick chemistry, regardless of the length of the linkers.

Establishing a Direct Assembly Approach for Rapid Construction of siRNA−tGalNAc Conjugates

Having confirmed the high efficiencies of the two-step coupling reactions, we then proceed to apply the strategy for the preparation of biologically relevant siTtr−tGalNAc conjugates that target the mouse *Ttr* gene (Figure 3a). Compared with the simpler model reactions using ssDNA, the conjugation for siRNA presents more challenges. First, the chemical compatibility of the linkers with siRNA must be carefully evaluated, as the PANAC photoclick chemistry has never been applied on siRNA molecules bearing backbone-containing thiol-rich phosphorothioate linkages before (Figure 3a).[5] Second, achieving high conversion yields while using lower equivalents of reagents is critical to ensure cost-efficiency for future drug substance manufacturing. While the conjugation is generally performed on a single strand (sense chain) prior to annealing with an antisense strand (preannealing conjugation),[13,18,19] which often requires high temperatures (e.g., up to 90 °C), this approach poses challenges when conjugating with heat-sensitive ligands such as proteins, antibodies, or aptamers. In such cases, extreme caution is needed to investigate the compatibility of the reaction conditions. Thus, we sought to perform the conjugation on annealed double-stranded siRNA (postannealing conjugation), to offer broader application scenarios.

To evaluate whether the tGalNAc−conjugation sites on siTtr molecules influence coupling efficiency and biological activities, we designed three siTtr molecules (Figure 3a) with amino-containing alkyl chains at different positions at 3′-ends of sense strands: 3′-OH of the last deoxythymidine (**siTtr1**) and the arms at C5 of deoxythymidines (dT) in the penultimate and last positions (**siTtr2** and **siTtr3**, respectively). The designed siTtr molecules were readily prepared via the standard protocol of solid-phase oligonucleotide synthesis with commercially available amine-containing dT building blocks and subsequently subjected to the two-step conjugation reactions (Figure 3b).

Compared to the ssDNA model reactions, we reduced the equivalents of linkers to 10-fold of siRNA (Table 1, entries 1−9, see Supporting Information Figures S2−S4, S6−S8 and S10−S12), and the reactions proceeded smoothly for all cases. In the large-scale (2 mM siTtr in 100 μL buffer as starting materials) preparation of siRNA conjugates for biological activity evaluation, we found that 5 equiv of linkers (10 mM) were sufficient to fully and cleanly convert 2 mM siRNA into desired amide products (Table 1, entries 10−16; entry 10 see Figure 3c and Supporting Information Figure S19; entries 11−16 see Supporting Information Figures S13−S18). After removal of excess linkers and buffer exchange by ultrafiltration, the siTtr-linker conjugates (1 mM) were directly subjected to coupling with 20 equiv of **tGalNAc-1** (20 mM) via PANAC photoclick chemistry using the same light activation condition as in ssDNA conjugation, with the conversion rates ≥90% in all cases (Table 2, entries 1−7; entry 1 see Figure 3c and Supporting Information Figure S19; entries 2−7 see Supporting Information Figures S13−S18). The reaction mixtures were then subjected to HPLC purification (separation yields in the range 51%−79%, Table 2) to remove small molecules for the following *in vivo* assessment of biological activities.

Table 1. Conversion of siTtr Molecules Reacting with Linkers[a]

Entry	siTtr	Linker	Conjugates	Conversion
1	siTtr1, 0.1 mM	Linker 1, 1 mM[b]	**siTtr1-Linker1**	>95%
2		Linker 2, 1 mM[b]	**siTtr1-Linker2**	>95%
3		Linker 3, 1 mM[b]	**siTtr1-Linker3**	>95%
4	siTtr2, 0.1 mM	Linker 1, 1 mM[b]	**siTtr2-Linker1**	>98%
5		Linker 2, 1 mM[b]	**siTtr2-Linker2**	>95%
6		Linker 3, 1 mM[b]	**siTtr2-Linker3**	>95%
7	siTtr3, 0.1 mM	Linker 1, 1 mM[b]	**siTtr3-Linker1**	>98%
8		Linker 2, 1 mM[b]	**siTtr3-Linker2**	>95%
9		Linker 3, 1 mM[b]	**siTtr3-Linker3**	>95%
10	siTtr1, 2 mM	Linker 1, 10 mM[c]	**siTtr1-Linker1**	>98%
11		Linker 3, 10 mM[c]	**siTtr1-Linker3**	>95%
12	siTtr2, 2 mM	Linker 1, 10 mM[c]	**siTtr2-Linker1**	>98%
13		Linker 2, 10 mM[c]	**siTtr2-Linker2**	>98%
14		Linker 3, 10 mM[c]	**siTtr2-Linker3**	>95%
15	siTtr3, 2 mM	Linker 1, 10 mM[c]	**siTtr3-Linker1**	>98%
16		Linker 3, 10 mM[c]	**siTtr3-Linker3**	>95%

[a]siTtr molecules and linkers at indicated concentration in reaction buffer were incubated at room temperature for 1 h. Since the retention times of the starting siTtr and siTtr-Linkers are very similar, the conversion was calculated based on MS analysis. [b]10 equiv. [c]5 equiv.

In each case, there is only one main peak in LC with no apparent signal of the single strand of siRNA, suggesting the coupling chemistries do not compromise the integrity of the structure of the double strand throughout the two-step process. In addition, the coupling efficiencies of each step of all cases are higher than 90%, even for producing the most sterically challenging **siTtr2-linker3-G** (featuring the structurally

https://doi.org/10.1021/jacsau.5c00012
JACS Au 2025, 5, 1402−1412

Table 2. Conversion of siTtr-Linkers Reacting with tGalNAc-1[a]

Entry	siTtr-linker	Conjugates	Conversion	Yield after HPLC purification
1	**siTtr1-Linker1**	**siTtr1-Linker1-G**	95%	73%
2	**siTtr1-Linker3**	**siTtr1-Linker3-G**	90%	51%
3	**siTtr2-Linker1**	**siTtr2-Linker1-G**	93%	69%
4	**siTtr2-Linker2**	**siTtr2-Linker2-G**	90%	59%
5	**siTtr2-Linker3**	**siTtr2-Linker3-G**	91%	70%
6	**siTtr3-Linker1**	**siTtr3-Linker1-G**	92%	66%
7	**siTtr3-Linker3**	**siTtr3-Linker3-G**	90%	79%

[a]The mixture containing siTtr-linkers (1 mM) and 20 equiv of tGalNAc (20 mM) in buffer (25 mM Na-Pi, pH 8.5) was transferred to a 96-well plate placed on ice and exposed to 365 nm irradiation at 10 mm distance for 15 min. The samples were collected and incubated at 25 °C for 1 h. Since the retention times of the siTtr-Linkers and the final siTtr−tGalNAc conjugates are very similar, the conversion was calculated based on MS analysis.

compact and rigid Linker 3 attached to the base of the internal nucleotide of **siTtr2**), highlighting the high efficiency of our method. Overall, we demonstrated high yield and clean conjugation of tGalNAc on double-stranded siRNA molecules in postannealing conjugation manner. Building on the high efficiency, mild conditions (i.e., room temperature and aqueous solution), and operational simplicity and practicality, we reason that our direct assembly strategy should be compatible with a broader range of ligands (e.g., protein, antibody, aptamer, etc.) for the future development of diverse oligonucleotide-based therapeutics.

Evaluation of siRNA−GalNAc Conjugate Activity in an Animal Model

We next evaluated the *in vivo* pharmacological properties of the prepared siRNA−tGalNAc conjugates (Table 2, entries 1−7) on the mouse model, compared with the parent conjugate **siTtr-P** as positive control (Figure 3a). The mRNA levels of *Ttr* were analyzed 5 days after subcutaneous administration of conjugates in three doses (0.5, 1.5, and 5 mg/kg) (Figure 4a). Compared to phosphate-buffered saline (PBS) treatment (negative control), the positive control **siTtr-P** exhibited dose-dependent efficacy and robustly suppressed the *Ttr* level (to 10.4%) at 5 mg/kg, which is similar to that previously reported.[27] (Figure 4b). At 0.5 and 1.5 mg/kg, **siTr1-Linker3-G** showed higher suppression activities on *Ttr* compared to **siTtr-P** (*Ttr* level, 41.8% vs 52.5%, $p = 0.029$; 29.2% vs 35.7%, $p = 0.018$), suggesting higher delivery efficiency to ASGPR. At high dose (5 mg/kg), most of the prepared siRNA−tGalNAc conjugates exhibited activities comparable to **siTtr-P**, with **siTtr2-Linker1-G** showing better activity (*Ttr* level, 7.7% vs 10.4%, $p = 0.012$). These results collectively indicated that our prepared siRNA−tGalNAc conjugates were efficiently delivered into the liver and translated into robust knockdown of *Ttr*, highlighting the effectiveness of our method for constructing siRNA−tGalNAc conjugates with strong *in vivo* pharmacological efficacies.

Advantages and Potential of the Direct Assembly Strategy for Constructing Ligand-Conjugated Oligonucleotides

Building on the above-mentioned experiments and results, our direct assembly strategy expands the toolkit for postsynthetic conjugation of oligonucleotide-based conjugates and therapeutics, offering several advantages: 1) Facilitation of SAR studies with accessible and diverse ligands of interest—the modular design of linkers and the sequential assembly of primary amines via amide coupling and PANAC photoclick chemistry enable the rapid assembly and screening of SARs using the same siRNA sequence backbone with diverse ligands of interest, thereby accelerating the optimization of conjugates for achieving enhanced biological activity;[2] 2) Accessibility and cost-effectiveness for constructing therapeutic oligonucleotides—unlike traditional solid-phase synthesis of ligand−siRNA conjugates requiring ligand-derived linkers that are preorganized on a solid support, variations in the ligands and their linkages require the use of a newly preassembled solid support for on-column synthesis of siRNA−ligand conjugates in each new SPS experiment,[17] while our strategy for direct

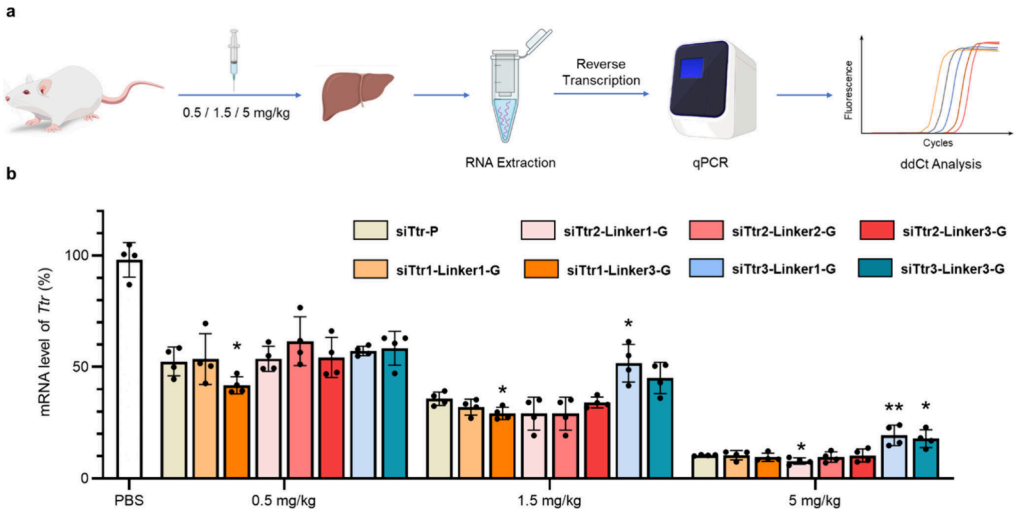

Figure 4. Evaluation of activities of prepared siTtr−tGalNAc in suppressing Ttr mRNA expression on a mouse model. a) Schematics of the workflow. b) Remaining mRNA level of Ttr 5 days after compound treatments. Statistical difference analysis was performed on the data of compounds against those of siTtr-P at the same dosage, using an unpaired two-tailed Students' *t* test ($n = 4$, * < 0.05, ** < 0.01).

https://doi.org/10.1021/jacsau.5c00012
JACS Au 2025, 5, 1402−1412

assembly of commercially available primary-amine-modified oligonucleotide with ligands of interest could offer diverse ligand−oligonucleotide conjugates with the same sequence oligonucleotide; 3) Versatility and potential for assembly of special ligands—due to mild reaction conditions (e.g., room temperature, aqueous solution) and the versatile ability to conjugate diverse primary amines of PANAC photoclick chemistry,[24−26,28−40] the direct assembly strategy can be applied to postannealing conjugation with a variety of potential heat-sensitive ligands (e.g., antibodies, proteins, and aptamers),[5] which preannealing conjugation strategies cannot accommodate. Collectively, the PANAC photoclick chemistry-enabled direct assembly strategy addresses key challenges in development of therapeutically relevant multifunctional oligonucleotide conjugates with conventional solid-phase synthesis and other in-solution postsynthetic methods. We believe our approach provides a robust and efficient platform for the development of oligonucleotide-based therapeutic agents.[2−5]

CONCLUSION

In this study, we developed a PANAC photoclick chemistry-enabled direct assembly strategy for the modular, efficient, and rapid construction GalNAc−oligonucleotide conjugates in solution, leading to enhanced *in vivo* potency. Through amide coupling of *o*-NBA-NHS modules with primary-amine-modified oligonucleotides, followed by conjugation of the primary amine of the tGalNAc moiety via PANAC photoclick chemistry, our method demonstrates the efficient and rapid assembly of therapeutically relevant oligonucleotides with ligands of interest, offering operational simplicity and practicality; thus, it effectively overcomes the limitations of existing methods. Moreover, importantly, the developed siRNA−tGalNAc conjugates exhibited comparable or superior *in vivo* antisense activity to the positive-control conjugate, highlighting the effectiveness of our strategy in rapidly and efficiently generating siRNA conjugates with robust pharmacological properties. Furthermore, the modular design of linkers and the sequential assembly of primary amines facilitate the rapid screening of structure−activity relationships (SARs) using commercially available primary-amine-modified oligonucleotides conjugated with diverse ligands of interest. This approach enables access to a wide variety of oligonucleotide−ligand conjugates, thereby accelerating optimization to enhance biological activity. Overall, our method expands the toolbox for preparing siRNA−tGalNAc conjugates, providing a general and efficient platform with broad applicability in constructing oligonucleotide conjugates, and thus would advance the development of oligonucleotide-based therapeutic agents to achieve desired pharmacological activity.

ASSOCIATED CONTENT

Supporting Information

The Supporting Information is available free of charge at https://pubs.acs.org/doi/10.1021/jacsau.5c00012.

Supplementary figures (S1−20) and LC-MS data for siTtr and conjugates. ^{1}H and ^{13}C NMR spectra for all linkers. Additional experimental details, materials, and methods (PDF)

AUTHOR INFORMATION

Corresponding Author

Xiao-Hua Chen − *State Key Laboratory of Drug Research, Shanghai Institute of Materia Medica, Chinese Academy of Sciences, Shanghai 201203, China; University of Chinese Academy of Sciences, Beijing 100049, China; School of Pharmaceutical Science and Technology, Hangzhou Institute for Advanced Study, University of Chinese Academy of Sciences, Hangzhou 310024, China;* orcid.org/0000-0003-3031-7095; Email: xhchen@simm.ac.cn

Authors

Hui-Jun Nie − *State Key Laboratory of Drug Research, Shanghai Institute of Materia Medica, Chinese Academy of Sciences, Shanghai 201203, China*

Hao Hu − *State Key Laboratory of Drug Research, Shanghai Institute of Materia Medica, Chinese Academy of Sciences, Shanghai 201203, China;* orcid.org/0000-0003-1365-0267

Xinming Qi − *Center for Drug Safety Evaluation and Research, Shanghai Institute of Materia Medica, Chinese Academy of Sciences, Shanghai 201203, China*

Yin-Jue Zhou − *State Key Laboratory of Drug Research, Shanghai Institute of Materia Medica, Chinese Academy of Sciences, Shanghai 201203, China; University of Chinese Academy of Sciences, Beijing 100049, China*

Lu Liu − *Center for Drug Safety Evaluation and Research, Shanghai Institute of Materia Medica, Chinese Academy of Sciences, Shanghai 201203, China*

Complete contact information is available at: https://pubs.acs.org/10.1021/jacsau.5c00012

Author Contributions

#H.-J.N., H.H., and X.Q. contributed equally to this work. CRediT: **Huijun Nie** data curation, formal analysis, investigation, methodology, validation, writing - original draft; **Hao Hu** data curation, formal analysis, investigation, methodology, validation, writing - original draft, writing - review & editing; **Xinming Qi** data curation, formal analysis, investigation, methodology, validation, writing - original draft; **Yin-Jue Zhou** formal analysis, investigation, validation; **Lu Liu** formal analysis, methodology, validation; **Xiao-Hua Chen** conceptualization, data curation, formal analysis, funding acquisition, investigation, project administration, supervision, writing - original draft, writing - review & editing.

Notes

The authors declare no competing financial interest.

ACKNOWLEDGMENTS

This study was supported by the National Science Foundation of China (No. 22377136 to X.-H. C.; 22377133 to H. H.).

REFERENCES

(1) Androsavich, J. R. Frameworks for transformational breakthroughs in RNA-based medicines. *Nat. Rev. Drug Discovery* **2024**, *23*, 421−444.

(2) Obexer, R.; Nassir, M.; Moody, E.; Baran, P.; Lovelock, S. Modern approaches to therapeutic oligonucleotide manufacturing. *Science* **2024**, *384*, No. eadl4015.

(3) Kulkarni, J. A.; Witzigmann, D.; Thomson, S. B.; Chen, S.; Leavitt, B. R.; Cullis, P. R.; van der Meel, R. The current landscape of nucleic acid therapeutics. *Nat. Nanotechnol.* **2021**, *16*, 630−643.

(4) Egli, M.; Manoharan, M. Chemistry, structure and function of approved oligonucleotide therapeutics. *Nucleic Acids Res.* **2023**, *51*, 2529−2573.
(5) Tang, Q.; Khvorova, A. RNAi-based drug design: considerations and future directions. *Nat. Rev. Drug Discovery* **2024**, *23*, 341−364.
(6) Jadhav, V.; Vaishnaw, A.; Fitzgerald, K.; Maier, M. A. RNA interference in the era of nucleic acid therapeutics. *Nat. Biotechnol.* **2024**, *42*, 394−405.
(7) Roberts, T. C.; Langer, R.; Wood, M. J. Advances in oligonucleotide drug delivery. *Nat. Rev. Drug Discovery* **2020**, *19*, 673−694.
(8) Hu, B.; Zhong, L.; Weng, Y.; Peng, L.; Huang, Y.; Zhao, Y.; Liang, X.-J. Therapeutic siRNA: state of the art. *Signal Transduct. Target. Ther.* **2020**, *5*, 101.
(9) Brown, C. R.; Gupta, S.; Qin, J.; Racie, T.; He, G.; Lentini, S.; Malone, R.; Yu, M.; Matsuda, S.; Shulga-Morskaya, S.; et al. Investigating the pharmacodynamic durability of GalNAc-siRNA conjugates. *Nucleic Acids Res.* **2020**, *48*, 11827−11844.
(10) Debacker, A. J.; Voutila, J.; Catley, M.; Blakey, D.; Habib, N. Delivery of oligonucleotides to the liver with GalNAc: from research to registered therapeutic drug. *Mol. Ther.* **2020**, *28*, 1759−1771.
(11) Dowdy, S. F. Overcoming cellular barriers for RNA therapeutics. *Nat. Biotechnol.* **2017**, *35*, 222−229.
(12) Seth, P. P.; Tanowitz, M.; Bennett, C. F. Selective tissue targeting of synthetic nucleic acid drugs. *J. Clin Invest.* **2019**, *129*, 915−925.
(13) Kandasamy, P.; Mori, S.; Matsuda, S.; Erande, N.; Datta, D.; Willoughby, J. L.; Taneja, N.; O'Shea, J.; Bisbe, A.; Manoharan, R. M.; et al. Metabolically stable anomeric linkages containing GalNAc-siRNA conjugates: an interplay among ASGPR, Glycosidase, and RISC pathways. *J. Med. Chem.* **2023**, *66*, 2506−2523.
(14) Nair, J. K.; Willoughby, J. L.; Chan, A.; Charisse, K.; Alam, M. R.; Wang, Q.; Hoekstra, M.; Kandasamy, P.; Kel'in, A. V.; Milstein, S.; et al. Multivalent N-acetylgalactosamine-conjugated siRNA localizes in hepatocytes and elicits robust RNAi-mediated gene silencing. *J. Am. Chem. Soc.* **2014**, *136*, 16958−16961.
(15) Matsuda, S.; Keiser, K.; Nair, J. K.; Charisse, K.; Manoharan, R. M.; Kretschmer, P.; Peng, C.G. V.; Kel'in, A.; Kandasamy, P.; Willoughby, J. L.; et al. siRNA conjugates carrying sequentially assembled trivalent N-acetylgalactosamine linked through nucleosides elicit robust gene silencing in vivo in hepatocytes. *ACS Chem. Biol.* **2015**, *10*, 1181−1187.
(16) Ulashchik, E. A.; Martynenko-Makaev, Y. V.; Akhlamionok, T. P.; Melnik, D. M.; Shmanai, V. V.; Zatsepin, T. S. Synthesis of galNAc-oligonucleotide conjugates using galnac phosphoramidite and triple-galNAc CPG solid support. *Design and Delivery of SiRNA Therapeutics* **2021**, *2282*, 101−118.
(17) Pon, R. T. Solid-phase supports for oligonucleotide synthesis. *Curr. Protoc Nucleic Acid Chem.* **2000**, DOI: 10.1002/0471142700.nc0301s00.
(18) Østergaard, M. E.; Yu, J.; Kinberger, G. A.; Wan, W. B.; Migawa, M. T.; Vasquez, G.; Schmidt, K.; Gaus, H. J.; Murray, H. M.; Low, A.; et al. Efficient synthesis and biological evaluation of 5′-GalNAc conjugated antisense oligonucleotides. *Bioconjugate Chem.* **2015**, *26*, 1451−1455.
(19) Tölke, A. J.; Gaisbauer, J. F.; Gärtner, Y. V.; Steigenberger, B.; Holovan, A.; Streshnev, F.; Schneider, S.; Müller, M.; Carell, T. Efficient Tandem Copper-Catalyzed Click Synthesis of Multisugar-Modified Oligonucleotides. *Angew. Chem., Int. Ed.* **2024**, *63*, No. e202405161.
(20) Engelhardt, D.; Nordberg, P.; Knerr, L.; Malins, L. R. Accessing Therapeutically-Relevant Multifunctional Antisense Oligonucleotide Conjugates Using Native Chemical Ligation. *Angew. Chem., Int. Ed.* **2024**, *63*, No. e202409440.
(21) Fantoni, N. Z.; El-Sagheer, A. H.; Brown, T. A hitchhiker's guide to click-chemistry with nucleic acids. *Chem. Rev.* **2021**, *121*, 7122−7154.
(22) Jayaprakash, K. N.; Peng, C. G.; Butler, D.; Varghese, J. P.; Maier, M. A.; Rajeev, K. G.; Manoharan, M. Non-Nucleoside Building Blocks for Copper-Assisted and Copper-Free Click Chemistry for the Efficient Synthesis of RNA Conjugates. *Org. Lett.* **2010**, *12*, 5410−5413.
(23) Malinowska, A. L.; Huynh, H. L.; Correa-Sánchez, A. F.; Bose, S. Thiol-Specific Linkers for the Synthesis of Oligonucleotide Conjugates via Metal-Free Thiol-Ene Click Reaction. *Bioconjugate Chem.* **2024**, *35*, 1553−1567.
(24) Guo, A.-D.; Yan, K.-N.; Hu, H.; Zhai, L.; Hu, T.-F.; Su, H.; Chi, Y.; Zha, J.; Xu, Y.; Zhao, D.; et al. Spatiotemporal and global profiling of DNA-protein interactions enables discovery of low-affinity transcription factors. *Nat. Chem.* **2023**, *15*, 803−814.
(25) Guo, A.-D.; Wei, D.; Nie, H.-J.; Hu, H.; Peng, C.; Li, S.-T.; Yan, K.-N.; Zhou, B.-S.; Feng, L.; Fang, C.; et al. Light-induced primary amines and o-nitrobenzyl alcohols cyclization as a versatile photoclick reaction for modular conjugation. *Nat. Commun.* **2020**, *11*, 5472.
(26) Hu, H.; Hu, W.; Guo, A.-D.; Zhai, L.; Ma, S.; Nie, H.-J.; Zhou, B.-S.; Liu, T.; Jia, X.; Liu, X.; et al. Spatiotemporal and direct capturing global substrates of lysine-modifying enzymes in living cells. *Nat. Commun.* **2024**, *15*, 1465.
(27) Nair, J. K.; Attarwala, H.; Sehgal, A.; Wang, Q.; Aluri, K.; Zhang, X.; Gao, M.; Liu, J.; Indrakanti, R.; Schofield, S.; et al. Impact of enhanced metabolic stability on pharmacokinetics and pharmacodynamics of GalNAc-siRNA conjugates. *Nucleic Acids Res.* **2017**, *45*, 10969−10977.
(28) Nie, H.-J.; Guo, A.-D.; Lin, H.-X.; Chen, X.-H. Rapid and halide compatible synthesis of 2-N-substituted indazolone derivatives via photochemical cyclization in aqueous media. *RSC Adv.* **2019**, *9*, 13249−13253.
(29) Yan, K. N.; Nie, Y. Q.; Wang, J. Y.; Yin, G. L.; Liu, Q.; Hu, H.; Sun, X.; Chen, X. H. Accelerating PROTACs discovery through a direct-to-biology platform enabled by modular photoclick chemistry. *Adv. Sci.* **2024**, *11*, 2400594.
(30) Li, J.; Hu, Q.-L.; Song, Z.; Chan, A. S.; Xiong, X.-F. Cleavable Cys labeling directed Lys site-selective stapling and single-site modification. *Sci. China Chem.* **2022**, *65*, 1356−1361.
(31) Hu, W.; Yuan, Y.; Wang, C.-H.; Tian, H.-T.; Guo, A.-D.; Nie, H.-J.; Hu, H.; Tan, M.; Tang, Z.; Chen, X.-H. Genetically encoded residue-selective photo-crosslinker to capture protein-protein interactions in living cells. *Chem.* **2019**, *5*, 2955−2968.
(32) Guo, A.-D.; Wu, K.-H.; Chen, X.-H. Light-induced efficient and residue-selective bioconjugation of native proteins via indazolone formation. *RSC Adv.* **2021**, *11*, 2235−2241.
(33) Suo, Y.; Li, K.; Ling, X.; Yan, K.; Lu, W.; Yue, J.; Chen, X.; Duan, Z.; Lu, X. Discovery small-molecule p300 inhibitors derived from a newly developed indazolone-focused DNA-encoded library. *Bioconj. Chem.* **2024**, *35*, 1251−1257.
(34) Wei, H.; Zhang, T.; Li, Y.; Zhang, G.; Li, Y. Covalent capture and selection of DNA-encoded chemical libraries via photo-activated lysine-selective crosslinkers. *Chem. Asian J.* **2023**, *18*, No. e202300652.
(35) Warminski, M.; Grab, K.; Szczepanski, K.; Spiewla, T.; Zuberek, J.; Kowalska, J.; Jemielity, J. Photoactivatable mRNA 5′ cap analogs for RNA-protein crosslinking. *Adv. Sci.* **2024**, *11*, 2400994.
(36) Bao, Y.; Xing, M.; Matthew, N.; Chen, X.; Wang, X.; Lu, X. Macrocyclizing DNA-Linked peptides via three-component cyclization and photoinduced chemistry. *Org. Lett.* **2024**, *26*, 2763−2767.
(37) Lu, D.-Q.; Liu, D.; Liu, J.; Li, W.-X.; Ai, Y.; Wang, J.; Guan, D. Facile synthesis of chitosan-based nanogels through photo-cross-linking for doxorubicin delivery. *Int. J. Biol. Macromol.* **2022**, *218*, 335−345.
(38) Li, M.; Liu, X.; Shang, J.; Wang, X.; Zhang, X.-B.; Xiong, B. Light-mediated protein functionalization of photoclickable hydrogel interface for selective cell capture and dot blotting assay. *Talanta* **2024**, *267*, 125248.
(39) Wang, J.; Qi, F.; Feng, H.; Xu, A.; Lu, D.-Q.; Liang, J.; Zhang, Z.; Li, J.; Liu, D.; Zhang, B.; et al. In situ formed tissue-adhesive carboxymethyl chitosan hydrogels through photoclick chemistry for wound healing. *Eur. Polym. J.* **2024**, *203*, 112680.

(40) Rizzo, R.; Barber, D. M.; Wilt, J. K.; Ainscough, A. J.; Lewis, J. A. Photoinitiator-free light-mediated crosslinking of dynamic polymer and pristine protein networks. *Biomater.Sci.* **2024**, *13*, 210−222.
(41) Spicer, C. D.; Pashuck, E. T.; Stevens, M. M. Achieving controlled biomolecule-biomaterial conjugation. *Chem. Rev.* **2018**, *118*, 7702−7743.
(42) Coelho, T.; Adams, D.; Silva, A.; Lozeron, P.; Hawkins, P. N.; Mant, T.; Perez, J.; Chiesa, J.; Warrington, S.; Tranter, E.; et al. Safety and efficacy of RNAi therapy for transthyretin amyloidosis. *New Engl. J. Med.* **2013**, *369*, 819−829.

https://doi.org/10.1021/jacsau.5c00012
JACS Au 2025, 5, 1402−1412